DOR: 20.1001.1.2322388.2019.7.3.5.1

Research Paper

The Effect of Magnesium on the Microstructure and Stress Rupture Properties of Hastelloy X Supealloy

Masumeh Seifollahi*, Afagh Panahi Moghaddam, Seyed Mahdi Abbasi, Seyed Mahdi Ghazi Mir Saeed

Malek Ashter University of Technology, Metallic Materials Research Center (MMRC_MA), Tehran, Iran.

ARTICLE INFO

Article history:

Received 23 April 2019
Accepted 4 July 2019
Available online 7 August 2019

Keywords:
Hastelloy X Superalloy
Magnesium
Microstructure
Stress Rupture Life

ABSTRACT

In the present study, the effects of magnesium on the microstructural characteristics and stress-rupture properties of the Hastelloy X superalloy were investigated. In this regard, four alloys with different amounts of magnesium (0, 17, 33, 47 ppm) were cast via the vacuum induction melting and then purified via the electro slag remelting. Microstructural observations were carried out through optical and scanning electron microscopes, and phase analysis was performed by X-ray diffraction. The stress rupture test was carried out at 815 °C/130 MPa. The results showed an almost significant effect of magnesium on decreasing grain size and sulfur content and increasing M_6C carbides volume fraction. Magnesium changed the morphology of carbides from the course and continue to finely divide one. Mg segregated at the grain and carbide boundary decreases the lattice parameters of the matrix and changes the composition of M_6C. Magnesium increased the rupture life by 46%. The most important causes for improving the rupture life of the Hastelloy X in the presence of magnesium are the increasing carbides volume fraction, improving its morphology, and decreasing sulfur content.

* **Corresponding author:**
E-mail address: m_seifollahi@mut.ac.ir

1-Introduction

Hastelloy X is a solid solution strengthening type nickel-based superalloy that possesses strong strength characteristics at elevated temperatures and excellent resistance to corrosion. It is well suited for forming and welding and uses in aircraft engine combustion chamber components [1,2]. Since the introduction of superalloys, the effect of grain boundary strengthening elements such as carbon, boron, zirconium, Hafnium and Magnesium on microstructure and researchers [3,4]. It has been reported [5-8] that small amounts of Mg addition to several wrought superalloys were enhanced the toughness, hot workability, creep life, and ductility of these alloys. Mg was found to segregate at the interface of the carbide/matrix, refine the primary MC carbide and inhibit the scriptlike carbide formation. The carbide characteristics at the grain boundary control the fracture mode of the Mar-M247 superalloy under creep conditions [5]. Investigations [4,6,9] showed that the addition of 1-350 ppm Mg to IN718 superalloy, 0-160 ppm to IN690, and 30-60 ppm to MAR-M247 increase the mechanical properties, but its effect and underlying mechanisms are not well understood in Hastelloy X. In steels, Mg contribute to heterogeneous ferrite nucleation during austenite decomposition and modifies microstructure [10,11]. Furthermore, magnesium is an alkaline earth metal element that has a strong reactivity with oxygen, sulfur, phosphorus, etc. The beneficial effects of magnesium on impurity removal from superalloys have been reported [2].

So far, many studies [2,12,13] have been performed on the enhancement of high-temperature mechanical properties of Hastelloy X superalloy by cold deformation and annealing treatment. With a review of related studies, it was observed that there is no research investigation about the effect of magnesium on the strengthening mechanisms of Hastelloy X superalloy. Therefore, the present study aims to investigate the effect of this element on microstructure characteristics and stress rupture properties of the Hastelloy X superalloy.

2. Experimental

Nickel-based superalloy Hastelloy X (20.80 Cr-20.2 Fe, 9.20 Mo, 1.70 Co, 0.80 W, 0.52 Si, 0.04 C, 0.37 Mn, 0.024 Nb, 0.03 V, 0.006 B) with different Magnesium content (0, 17, 33 and 47 ppm) was cast via the vacuum induction melting (VIM) and then purified via the Electro Slag remelting (ESR). The alloy designations are 0Mg, 17Mg, 33Mg, and 47Mg. The furnace was evacuated to 10 -3 pa and purged with high purity argon. All raw materials were rinsed separately with acetone and charged into a MgO-Al_2O_3 crucible, but Al, B, Mn, and Mg were charged after the full melting of the charged materials. The pouring temperature was 1350±20 °C. As a secondary melting process, electro-slag remelting was undertaken with a flux of 60% CaF_2–20% Al2O3–16% CaO–4%TiO_2. Cast ingots were homogenized at 1200 °C for 4 h and subsequently hot-rolled at 1100 °C to a reduction of 83%.

Chemical composition determined using Spark Emission Spectrometer quantometry method. Mg and S contents were measured using ICP-OES 730 and LECO-CS 244 apparatus, respectively. A Phillips PW 1800 X-ray diffractometer (40 kV, 30 mA) with CuKα radiation was used for X-ray diffraction (XRD) and phase identification. Metallographic sections were prepared using standard mechanical polishing procedures and etched using kalling's waterless solution. A Vega Tescan scanning electron microscope (SEM) with an energy dispersive spectroscopy (EDS) analysis operating at 15 kV and optical microscopy were used to examine the morphology and distribution of the phases. The volume fraction of phases and grain size was calculated using Clemex image analysis software on the basis of ASTM E562 and E112 standards.

The stress-rupture test of the sub-sized specimens (with a gauge section of 15×6.25×1.25 mm) was carried out at 815 °C/130 MPa in air. At least two specimens were tested under the same conditions according to ASTM E139-11 standard.

3. Results and Discussion

3.1. Phase constitution and microstructure of the alloy

The XRD Patterns of the 0Mg and 47Mg alloys are shown in Fig. 1. As it can be seen, the peaks pertaining to ɤ matrix and M_6C carbides are evident in both alloys. It was observed that Mg caused the peaks to shift towards higher angles. Considering the inverse ratio of x-ray diffraction angle to the distance between crystalline planes according to Bragg rule ($n\lambda=2d\sin\theta$) and also the direct relationship between the lattice constant and distance of crystal planes for the cubic systems ($\frac{1}{d^2}=\frac{h^2+k^2+l^2}{a^2}$), it can be concluded that Mg increased the X-ray angle and reduced the matrix lattice parameters from 3.60 to 3.58 A. The shift in XRD peak is the result of changes in lattice parameters differences between Mg and Ni atomic size. The atomic radii of Mg and Ni are 1.96 Å and 1.63 Å respectively [14]. Furthermore, in the presence of magnesium, the intensity of the M_6C phase peak and the peak width increased. Moreover, the peak height ratios of Gamma/M_6C decreased from 3.211 to 3.000 by adding 47 ppm Mg. Therefore it can be concluded that magnesium increased the volume

fraction and the lattice constant of the M_6C phase. The M_6C phase will be discussed in the microstructure section.

The optical microstructures of all four samples (Fig. 2) indicated the γ grains, twins, and carbide phases. SEM images of alloys in Fig. 3 also revealed the presence of carbide inside the grains and on their boundaries. According to Figs. 2 and 3, magnesium can affect grain size, volume fraction, size, and morphology of carbides. Variations in grain size and carbide volume fraction are shown in Fig. 4. An increase in Mg content from 0 to 47 ppm resulted in the decline of the grain size from 64 to 38 μm; the average carbide size also decreased from 3.77 to 2.1 μm; while the carbide content increased from 2.2 to 4.6%. Furthermore, according to Fig. 3, 0Mg samples exhibited the coarse and continuous carbides, while the carbides were finely distributed in the presence of magnesium. During the solidification of Mg-doped alloy, tiny and distinct carbides were formed, which acted as nucleation sites and decreased the grain size. In addition, due to the differences in the atomic size of magnesium (1.96) and the matrix (1.69), magnesium was slightly soluble in the matrix, so it segregated at the grain boundaries and prevented from the boundary movement during hot rolling giving rise to grain size reduction. One of the annealing-induced changes is the formation of new equiaxed and stress-free grains in the alloy. Microstructural investigation shows that at the presence of 47 ppm Mg, complete recrystallization occurred, and fine grain structure was achieved.

Chemical compositions (analyzed by EDS) of different regions included matrix and carbides of 0Mg, and 47Mg samples are summarized in Table 1 and Fig. 5. The carbide forming elements include carbon, molybdenum, iron, nickel, tungsten, and chromium in both samples, which were more than the other elements. According to XRD results in Fig. 1, the carbide was of M_6C type, usually known as initial M_6C carbides. It is worth noting that according to EDS analysis and TTT graph [5], $M_{23}C_6$ carbide can't form in these temperatures and times.

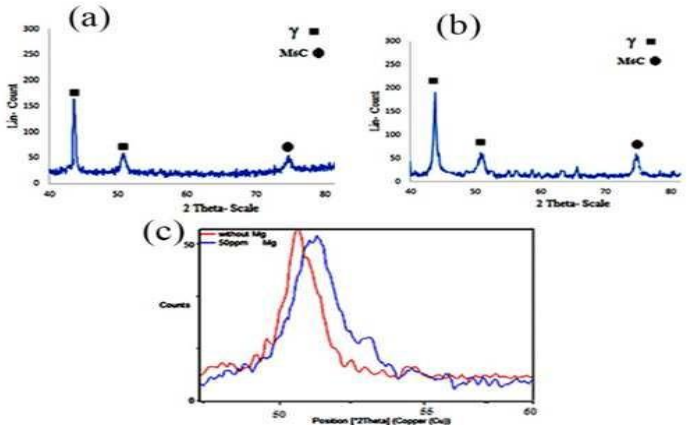

Fig. 1. The XRD pattern of Hastelloy X, a) 0Mg, b) 47 Mg and c) comparison of matrix peak.

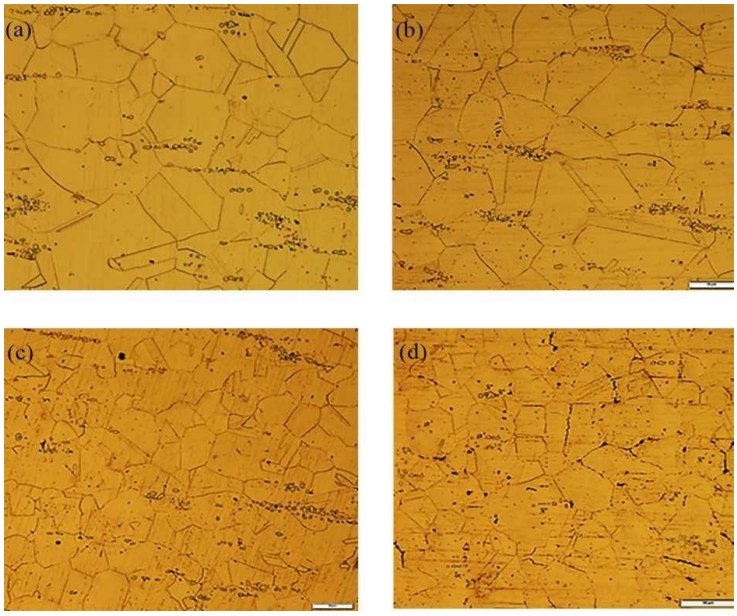

Fig. 2. Microstructure of Hastelloy X heat treated at 1175 °C, a)0Mg, b)17Mg, c) 33Mg, d) 47Mg.

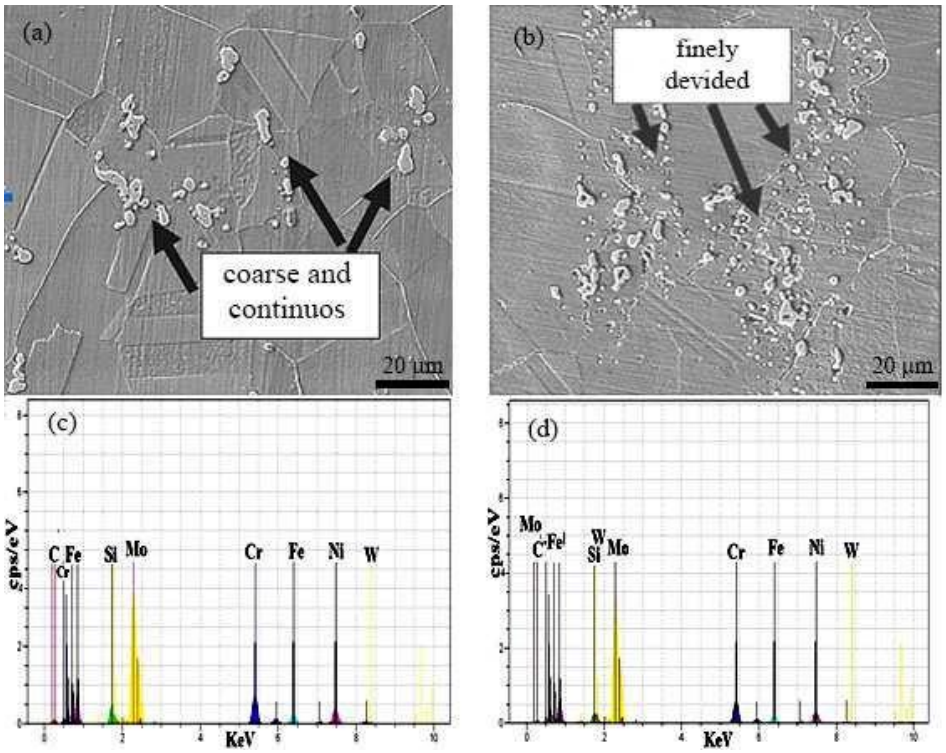

Fig. 3. SEM microstructure and EDS spectrum of Hastelloy X heat treated at 1175 °C; a and c) 0Mg; b and d) 47Mg

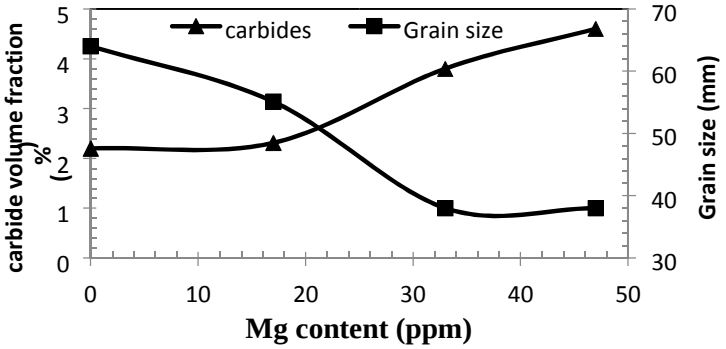

Fig.. 4. The curves of carbide volume fraction and grain size variation versus Mg content in Hastelloy X.

.

EDS analysis and line scan of carbides in Table 1 and Fig. 5 show that molybdenum and tungsten content of carbide increased from 43.09 and 0.10 wt% in 0Mg sample to 54.55 and 8.09 wt% in 47Mg, respectively. Soluble magnesium in the carbide and the matrix may change the chemical composition and affect the transfer of carbon and carbide forming elements (Mo and W). Magnesium seems to affect the diffusion and transfer of these elements, as well as carbon, due to its higher atomic radius compared to molybdenum and tungsten. In other words, the formation of the Mg-rich layer in the carbide/matrix interfaces was effective on the transfer of carbon and the carbide-forming elements. This Mg-rich layer reduced the diffusion of these elements to the matrix and increased their concentration (C, Mo, and W) in the carbides. Mg segregation in carbide/matrix interface also prevented the formation of large carbides and caused a reduction in carbide size. Moreover, the reduction of molybdenum solubility, which is the main ingredient of M_6C, increased the carbide volume fraction. The changes in the chemical composition of carbide could also be due to the alternations in the lattice parameters of the matrix and the M_6C carbide according to the XRD test (Fig. 1). As it was mentioned before, comparing Fig. 1a and b, magnesium decreased the width of carbide M_6C peak while increasing its intensity. As a result, magnesium enhanced the carbide lattice parameters due to an increase in molybdenum dissolution.

3.2. The effect of magnesium on the rupture time of Hastelloy X Superalloy

Fig. 6 shows the time-strain curves of 0Mg, 33Mg, and 47Mg samples. According to Fig. 6, the first stage of creep (where the creep rate decreases) was short for all samples due to the high temperature and stress of the test. The second stage of creep showed an almost constant creep rate. The fixed strain rate of the second step identifies the stable microstructure. As it is shown in Table 3, the minimum creep rate of the 0Mg sample was more than 47Mg. The third and final creep stage involves the sample rupture accompanied by nucleation and growth of microcracks as the result of porosity. 0Mg sample exhibited a short third stage. The metals fail due to recrystallization, formation of cracks, and internal cavities [15]. As the second region creep time of the 47Mg sample was significantly higher than that of the 0Mg sample, it can be concluded that incorporation of 47 ppm Mg can result in good properties.

Table 1 Chemical composition of matrix and carbides in 0Mg and 47 Mg

sample	C	W	Fe	Mo	Cr	Ni	region
0Mg	0.90	0.83	19.40	8.05	21.90	45.00	**Matrix (wt%)**
	30.96	1.97	6.62	20.10	16.06	23.53	**Carbides (at%)**
47Mg	0.90	0.83	18.71	13.32	19.31	46.20	**matrix**
	20.70	0.03	18.24	28.21	16.68	16.14	**Carbides (at%)**

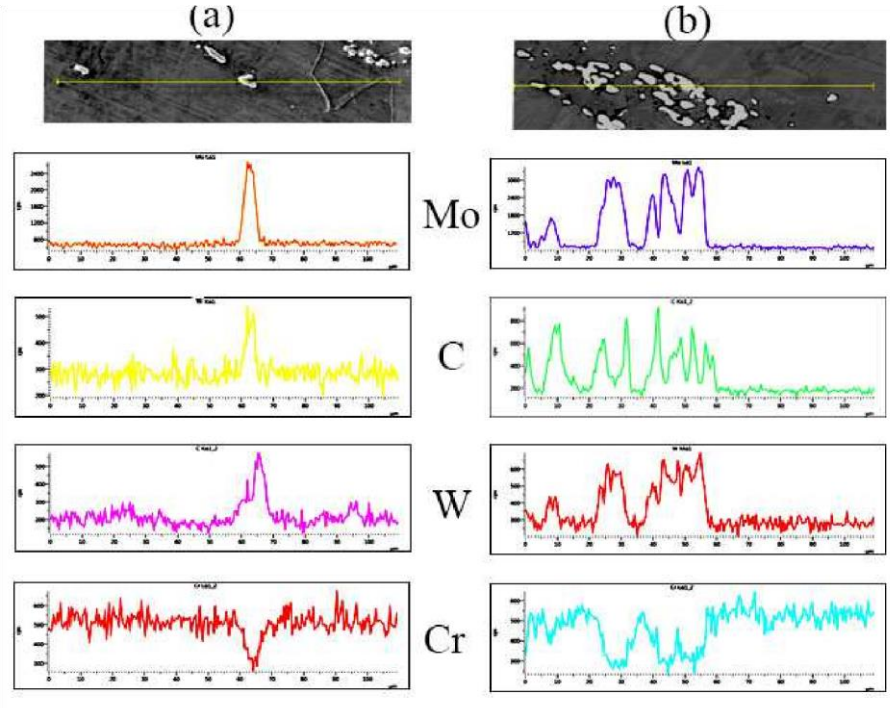

Fig. 5. EDS Line scan of carbides in a)0Mg and b)47Mg samples.

Table 2 Sulfur content of Hastelloy X doped by Mg

Sample	0Mg	17Mg	47Mg
Mg (ppm)	0	33	47
S (ppm)	94	88	70

Table 3 The minimum creep rate of Hastelloy X samples.

Sample	0Mg	17Mg	47Mg
Minimum creep rate (mm/s)	0.60×10-4	0.48×10^{-4}	0.22×10^{-4}

The reasons for the increase of rupture life by Mg incorporation are summarized below:

In spite of grain refinement by the addition of Mg, the increased volume fraction of carbides acted as a barrier for the motion of dislocations and increased the strength of superalloy. Carbides can withstand slippage and grain boundaries migration during the creep process.

a) Filling vacancies and b) reducing the grain boundaries diffusional as a result of minor element segregation on grain boundaries are the other two mechanisms for increasing rupture life in 47Mg specimen.

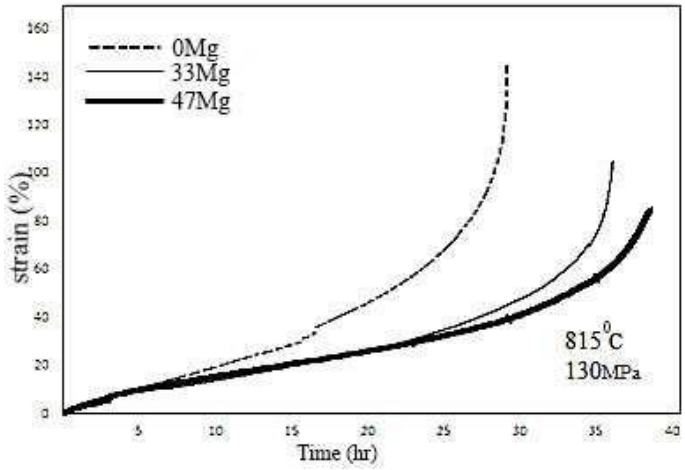

Fig. 6. Time-Strain curves obtained from stress rupture test at 815 °C/130 MPa of Hastelloy X doped by Mg.

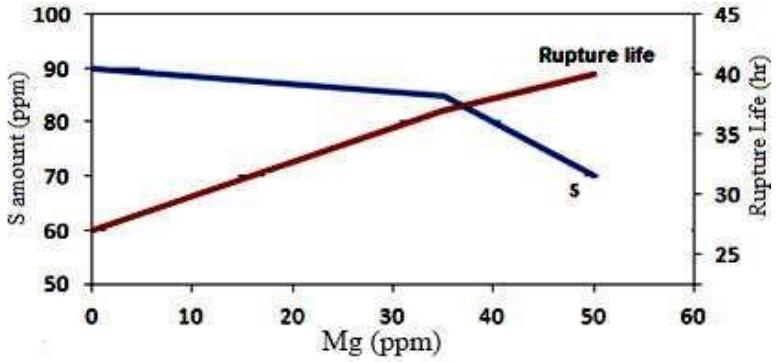

Fig. 7. Rupture life versus S and Mg content curves of the Hastelloy X doped by Mg

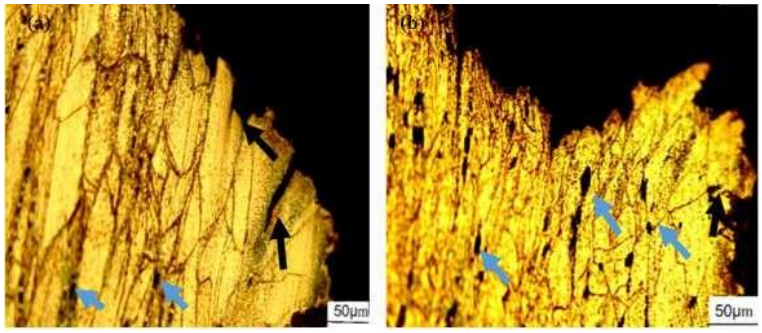

Fig. 8. Fracture surface of a)0Mg and b)47Mg samples after stress rupture test at 815 °C/130 MPa.

Magnesium reduced the density of vacancies in the boundary because of its large atomic radius. It has been reported [6] that Mg segregation on the boundary could cause deformation and stress concentration on the boundaries. As a result, nucleation and crack propagation will be delayed, and the rupture life and elongation will increase. Mg doping caused an incensement in the starting time of the creep crack nucleation, and propagation grain boundaries are degraded and separated in nickel-base superalloy along the interface area [16]. Changes in the At high temperatures, usually due to rupture life versus sulfur content, are shown segregation of impurities such as sulfur, the in Fig. 7. Consequently, an increase of Mg and reducing sulfur contents can significantly improve creep life and creep ductility. The fracture surfaces of 0Mg and 47Mg specimens are shown in Figs. 8a and b. Intergranular creep failure consists of nucleation, growth, and interconnecting of wedge-shaped cavities in the triangular boundaries, which is formed by the grain boundary sliding [17]. In 47Mg samples, the formation of cavities in triangular points was minimized; as it is seen, the fracture path was intragranular.

Owing to its larger atomic size, Mg segregated at the grain boundaries and reduced the concentration of vacancies. It consequently decreased the diffusion coefficient of the alloy. The initiation and propagation of creeping cavities were also reduced by decreasing the diffusion coefficient [17,18]; therefore, the magnesium segregation delayed the initial propagation of the cracks, minimized the formation of cavities in the triple points, and thus increased the failure time in intragranular mode.

4. Conclusion

Based on the finding of this study, these conclusions can be made:

1. Mg doping of Hastelloy X can decrease and increase the matrix and carbides lattice parameters, respectively, due to its atomic size and changing the carbide's chemical composition.
2. At the presence of Mg, the morphology of carbides changed from coarse and continuous structure to finely divided distribution.
3. Increase in magnesium content from 0 to 47 ppm decreased the grain size from 64 to 38 μm, the average carbide size was also decreased from 3.77 to 2.1 μm. The carbide content, however, increased from 2.2 to 4.6%. 4. Mg doping of Hastelloy X increased the rupture life due to changes in carbide size and morphology as well as sulfur removal from the alloy.

References

[1] L. M. Pike, "100+ years of wrought alloy development at haynes international", in 8th International Symposiumon Superalloy 718 and Derivatives, TMS, 2014, 15-30.

[2] Y. ming, N. yujing, "study on nonequilibrium grain-boundary segregation of sulfur among Hastelloy X", Adv. Mat. Rese., Vol. 181-182, 2011, pp. 861-865.

[3] H. Tsuji, T. Shimizu, S. Isobe, H. Nakajima, "Effect of minor alloying elements on hotworkability of Ni-Cr-W superalloys", j. Nucl. Sci. Tech., Vol. 31, 1994, 32-39.

[4] S.Yamaguchi, H. Kobayashi, T. Matsumiya, S. Hayami, "Effect of Minor Elements on Hot Workability of Nickel-Base Superalloys", Met. Tech., Vol. 6, 1979, pp. 170-175.

[5] H. Bor, C. Chao, C. Ma, "The Influence of Magnesium on Carbide Characteristics and Creep Behavior of The Mar-M247 Superalloy", Scripta Mater., Vol. 38, 1997, pp. 329-335.

[6] K. Banerjee, "The Role of Magnesium in Superalloys—A Review", Mat. Sci. Appl., Vol. 2, 2011, pp. 1243-1248.

[7] Z. X. xie, G. Chen, "The Role of Mg on Structure and Mechanics Properties in Alloy 718" , Metall. Society, 1988, pp. 635-642. [8] Y. Azakli, M. Tarakci M., "Towards understanding the effects of magnesium addition on microstructural and thermal properties of NiAlCr alloys in as-cast and heat treated states", j. alloys comp., Vol. 699, 2017, pp.151-159.

[9] H. Bor, C. Chao, C. and Ma, "The Effects of Mg Microaddition on the Mechanical Behavior and Fracture Mechanism of Mar-M247 Superalloy at Elevated Temperatures", Metall. Mat. Trans. A, Vol. 30, 1999, pp. 551-561.

[8] X. L. M. Lv, Y. Min, C. Liu, M. Jiang, B. Wang, X. Wang, "Effect of Trace Magnesium Addition on the Characteristics of Mechanical Properties in High Strength Low Alloy Steel", Advances In Engineering Research, 2015, pp.1-8.

[9] K. Kimura, S. Fukumoto, G. I. Shigesato, A. Takahashi, "Effect of Mg Addition on Equiaxed Grain Formation In Ferritic Stainless Steel", Isij Int., Vol. 53, 2013, pp. 2167-2175.

[10] H. Tawancy, "Long-Term Ageing Characteristics of Hastelloy Alloy X", J. Mat. Sci., Vol. 18, 1983, pp. 2976-2986.

[11] M. Aghaie-khafri, N. Golarzi, "Dynamic and Metadynamic Recrystallization of Hastelloy X Superalloy", J. Mat. Sci., Vol. 43, 2008, pp. 3717-3724.

[12] S.S. Batsanov, "Van der waals radii of elements", Inorganic Mat., 2001, vol. 37, pp.871–885.

[13] G. chen, D. wang, Z. Xu, J. Fu, K. Ni, X. Xie, "The role of small amounts of Magnesium in Nickle-base and Iron-Nickle-base superalloys after high temperature long time exposures", in superalloys , TMS, 1984, pp.611-620. [16] J. X. Dong, X. S. Xie, R. Thompson, "The influence of sulfur on stress-rupture fracture in inconel 718 superalloys", Metall. Mate. Trans. A, Vol. 31, 2000, pp 2135–2144.
[14] S. Jonas, M. Lundberg, H. Brodin, J. Moverare, "Dwell-fatigue crack propagation in additive manufactured Hastelloy X", Mat. Sci. Eng. A, Vol. 722, 2018, pp. 30-36.
[15] M. Kirka, R. Dehoff, "Mechanical Properties of Hastelloy X Fabricated by Electron Beam Melting", in Materials Science & Technology conf., Salt Lake City, UT, October 23-27, 2016.